

Cooling rates of mild steel welds during gmaw process made at different positions

J. I. Achebo

Department of Production Engineering, University of Benin, Benin City, Edo State, Nigeria

Abstract

This paper is aimed at examining the cooling rates of mild steel welds made at different welding positions, being the horizontal, vertical and overhead positions. The cooling rate affects the microstructure of the weld metal and in turn the microstructure determines the quality of the weld. Therefore the welding position which produces the weld with the best microstructural view is examined. Both experimental and computational methods are used for analyzing the problem statement. From the results obtained in this study, it was found that the cooling rates at the horizontal, vertical and overhead positions are 4.77°C/s, 4.99°C/s and 8.72°C/s respectively. From the microstructural analysis of the weld, it is found that the microstructure of the weld made at the horizontal position is of the best quality with minute to no trace of gas entrapment. The grains size from the microstructural view appears to be small and paste like, which indicates that the weld texture is very smooth. From this study, it has been shown that welding in the horizontal position when using Gas Metal Arc Welding (GMAW) process produces a weld of good quality microstructure.

Keywords: Cooling rates; microstructure; GMAW; HAZ; welding positions

1. Introduction

Weld microstructure is a vital component that defines the quality of a welding process. The state and quality of the microstructure is significantly affected by the heat input and the cooling rate. Yang and Debroy (1999) wrote that the heat and fluid flow in the weld pool affects its shape and size, cooling rate, and the resulting microstructure. Several researchers have reported that the cooling rate could greatly affect the microstructure of the weldment (Bhadeshia and Svensson, 1993; De et al. 2003).

Poorhydari et al. (2005) wrote that for a typical arc weld thermal cycle, rapid heating and fast cooling to ambient temperature occurs and that the microstructural changes in the weld zone are greatly affected by the heating and cooling rates. De et al. (2003) were of the opinion that the microstructure and properties of the weld metals is greatly affect by the cooling rate.

The method of cooling also has a determinable impact on the microstructure of the weld. This could either be by forced cooling, which involves cooling by quenching the weldment with oil or water, or normal cooling in still air. Forced cooling can result in the formation of internal stresses in the weld resulting to stress concentrations. These stress concentrations tend

to prevent uniform circulation of heat flow in the weld metal, in turn leading to a porous microstructure. The porous microstructure results from the inability of the grains to move from one region to another region creating cavities between the grain boundaries. Weld gasses occupy these cavities which upon cooling eventually become pores. A microstructural view of the weld would show that the grains that make up porous weld are large and cannot easily overlap making for poor cohesion, reducing its load bearing capacity and concomitantly increasing its susceptibility to unanticipated weld failure.

However, if the metal is allowed to cool in still air, the rate of cooling is gradual and the microstructure of the weld metal is not altered. The major limitation of this type of cooling process is that, it takes a much longer time to cool than with the forced cooling process.

In this study, the cooling rates of between 800°C and 500°C were considered. This temperature range has been considered by most investigators working on the cooling rates of ferrous materials. The reason for using this temperature range was given by De et al. (2003). The authors reported that a useful comparison of the cooling curves can be made by calculating t_{8-5} , the time taken for the weld pools to cool from 800°C to 500°C.

The authors emphasized that this is significant since it corresponds to the temperature regime over which austenite to ferrite phase transformations take place.

The models and methods used by Poorhaydar, et al. (2005) are adopted for this study. There are other investigators who have studied the cooling rates of weld metals. Hess et al (1943) measured the cooling rates of weld metals during the arc welding process using optimized process parameters. Rosenthal (1946) predicted the cooling rates of welds based on the assumption of a moving point heat source on the surface of the plate. Yang and Debrou (1999) determined the cooling rates of steel during the gas metal arc welding (GMAW) process. Atkins et al (2002) determined the cooling rates of steel when they were evaluating the fusion zone hydrogen induced cracking susceptibility of single pass weld deposits. De et al. (2003) predicted the cooling rates and the associated effects on microstructure in laser spot welds. Poorhaydari et al. (2005) estimated the cooling rates of steel plates using the model postulated by Rosenthal(1946).

In this research work, the effect of molten weld metal cooling rate on weld microstructure is examined.

2. Materials and methods

A GMAW machine was used to make weld deposits on mild steel plates measuring 40mm x 120mm x 8mm in dimension. The welding process took place in three welding positions. These are the horizontal, vertical and overhead positions. The parameters used for the experiment in these positions are shown in Table 2. After the welding process and the weld pool has cooled, the chemical composition of all weld metal was investigated using the spectrometer.

2.1. Weld metallurgical microscope

An Econet 11 weld metallurgical microscope was used. It is a digital microscope used to physically examine and take the microstructural view of the weld specimen to about one hundred times magnification.

The specimen is placed on a flat optical instrument whose reflections are captured by the lens. The microscope contains an adjustable lens that is used to bring the microstructural view of the specimen to focus, before pressing the nub which takes the photograph of the weld sample, physically showing the microstructure view of the weld which is contained in a film. The film undergoes some developmental treatment to produce the pictures showing these views. These views should reveal cracks and pores if present in the weld structure, which pores cannot be seen with the ordinary human eye. Under such magnification, the microstructure arrangement of the weld grains is also visualized (Achebo, 2008).

2.2. Theoretical models

In determining the cooling rate of mild steel plates, from 800°C to 500°C, the Rosenthal Equations for thick plates, earlier applied by Poorhaydari et al (2005), are similarly adopted in this study.

Equation (1) shows the intermediate temperature gradient occurring in the welding process:

$$T - T_0 = \frac{q/v}{2\pi\alpha t} \exp\left(-\frac{r^2}{4\alpha t}\right) \quad (1)$$

The cooling time from 800°C to 500°C is expressed in Eq(2)

$$\Delta t_{8-5} = \frac{q/v}{2\pi\alpha\theta_1} \quad (2)$$

Where

$$\frac{1}{\theta_1} = \left(\frac{1}{500 - T_o} - \frac{1}{800 - T_o} \right) \quad (3)$$

Where, T_0 = initial temperature = 227°C, λ = thermal conductivity = 44.26 Js⁻¹m⁻¹°C⁻¹, a = Thermal diffusivity = $\frac{\lambda}{\rho c} = 8.584 \times 10^{-6}$ m²/s

e = specific heat per unit volume = 425 J kg⁻¹°C⁻¹, specific heat of solid = 678.42 J kg⁻¹°C⁻¹, density, ρ = 7600 kg/m³ and q/v = heat input, J/s or Watts.

For electric arc welding, the heat input is written as

$$q/v = \frac{E.I.\eta}{v} \quad (4)$$

Where, E = arc voltage, V; I = arc current, A and η = arc efficiency, %.

Poorhaydari et al (2005) said that thermal or arc efficiency is lower than I, because some part of the arc energy is dissipated to the surroundings by radiation, convection, or conduction, and is therefore lost.

On the welding plate, the portion where temperature is expected to be highest is the heat affected zone (HAZ), whose width, W is defined in Eq (5).

$$\text{HAZ width, } W = C_1 \cdot (q/v)^{\frac{1}{2}} \quad (5)$$

$$C_1 = \left[\frac{2}{\pi e \rho c} \right]^{\frac{1}{2}} \cdot \left[\frac{1}{(A_1 - T_0)^{\frac{1}{2}}} - \frac{1}{(T_s - T_0)^{\frac{1}{2}}} \right] \quad (6)$$

Where A_1 is the lower critical temperature upon heating. This has been numerically expressed by Ion et al (1984) as

$$A_1 = 996 - 30\text{Ni} - 25\text{Mn} - 5\text{Co} + 25\text{Si} + 30\text{Al} + 25\text{Mo} + 50\text{V} \quad (7)$$

To determine A_1 , the values in Table 1 are substituted into Eq. (7)

Table 1
Chemical composition of mild steel weld

Element(%)	C	Mn	P	Ni	S	Cr	Si
Weldment	0.29	0.23	0.23	0.021	0.10	0.09	0.31

The alloying elements present in Eq (8) is measured in % by weight. A_1 is measured in %. Having determined the above parameters, the mean cooling rate for the temperature range of 800°C to 500°C is calculated in °C/s and expressed in Eq (8).

$$T_{800-500} = \frac{300}{\Delta t_{s-5}} \quad (8)$$

3. Discussion of results

Welding was carried out in three positions these are the horizontal, vertical and overhead positions. The relevance of this study, is to determine the cooling rates at this positions, which would further determine the convection-conduction modes of the welding process and determine the welding position that produces the weld with the best microstructure. Parameters used for this study are presented in Table 2.

Table 2
Parameters used in the study

Horizontal Position
Welding time, $t = 20s$
Welding voltage, $E = 10 - 12V$
Welding current, $I = 190 - 240A$
Radial/lateral distance from the weld = 0.004m
Welding speed, $V = 0.0065 - 0.0119 \text{ m/s}$
Arc efficiency, $\eta = 80\%$ (Okui et al, 2007).
Vertical Position
Welding time, $t = 26s$
Welding voltage, $E = 10 - 10V$
Welding current, $I = 120 - 155A$
Radial/lateral distance from the weld = 0.006m
Welding speed, $V = 0.0035 - 0.0055 \text{ m/s}$
Arc efficiency, $\eta = 75\%$ (Okui et al, 2007).
Overhead Position
Welding time, $t = 30s$
Welding voltage, $E = 10 - 11V$
Welding current, $I = 170 - 200A$
Radial/lateral distance from the weld = 0.0035m
Welding speed, $V = 0.0080 - 0.0150 \text{ m/s}$
Arc efficiency, $\eta = 70\%$ (Okui et al, 2007).

The cooling process of interest to this study is from the range of 800°C to 500°C. In the horizontal position, GMAW with a heat input of 1.9kW was used to make weld deposits. A preheating of the pieces of metals to be welded was made at 227°C. As the electrode is heated, it melts and forms a pool of molten metal, known as the weld pool at a temperature of 1825.89°C. The molten metal became solid before it got

to 800°C as it cooled in still air. As it cooled from 800°C to 500°C, the cooling time calculated was 62.84s and the corresponding cooling rate is 4.77°C/s. The width of the heat affect zone, HAZ, surrounding the weld pool is $8.5 \times 10^{-5} \text{ m}$.

For the vertical position, the electrode and the base metal were preheated to a temperature of 227°C using a GMAW machine with a heat input of 0.98KW. The weld pool was formed at a temperature of 1511.65°C. The cooling process occurred in still air to a temperature of 800°C. and the time it took to cool from 800°C to 500°C was 66.77s. The corresponding cooling rate was 4.49°C/s and the width of the HAZ, determined was $6.53 \times 10^{-5} \text{ m}$.

For the overhead position, the electrode and base metal were preheated to a temperature of 227°C. The electrode was heated with a GMAW machine which generated a heat input of 1.30KW until a temperature of 817.34°C was reached. The value of this temperature, although not enough to completely form a weld pool may have been affected by a highly aerated environment. Most workshops have their windows placed close to the roof and this makes the exchange of air and weldment very high. It took the weldment 34.41s to cool from 800°C to 500°C at a rate of 8.72°C/s and the width of the HAZ, is $-2.86 \times 10^{-5} \text{ m}$. The negative sign indicates that the HAZ is highly constricted and affected by the atmospheric air. Therefore, it is more of the conduction mode, that is, the cooling rate is very rapid and the boundary layers are cooled.

This also indicates that the welding process in both the horizontal and vertical positions generated a convection mode. This is the reason, the weld pools were formed at higher temperatures.

Other investigators also researched on the cooling rates of steel plates. Poorhaydar et al. (2005) used a nominal heat inputs of 0.5 KJ/mm, 1.5KJ/mm and 2.5 KJ/mm to weld a 1.2mm, 3.6mm and 5.9mm steel plates and a cooling time of 2.6s, 23.6s and 65.6s were determined with a corresponding cooling rate of 178.8°C/s 20.2°C/s and 7.8°C/s respectively.

Atkins et al. (2002) determined the cooling rates of steel plates using various welding processes for GMAW-S at heat inputs of 20KJ/in and 40KJ/in, and obtained cooling rates of 116F/s and 70F/s respectively. Using the SMAW process, at heat inputs of 20KJ/in and 40KJ/in, they obtained cooling rates of 100F/s and 60F/s respectively. The SAW process, at heat-inputs of 20KJ/in and 40KJ/in, gave cooling rates of 83F/s and 40F/s respectively.

Yang and Debroy (1999) used GMAW for welding HSLA-100 steels and calculated average cooling rates of 18.2, 22.2 and 28.6 K/s for welds 1,2 and 3, at temperatures between 1073 and 773K, with corresponding cooling times of 16.5, 13.5 and 10.5 seconds for welds 1,2 and 3. Yang and Debroy (1999) emphasized that the thickness of the HAZ varied spatially.

De et al. (2003) predicted the cooling rates of steels using the laser spot welding machine. At laser

power of 1.0kW and 1.4kW, the cooling rates are 9.0×10^{-5} and 7.0×10^{-5} K/s obtained with a temperature of 1400°C with cooling time of 0.15s and 2.65s respectively and also with a laser power of 2.23kW at 1400°C , a cooling rate of 2.8×10^{-5} K/s was obtained.

Figures 1,2 and 3 are 100×100 magnified microstructural views of weld deposits made in different positions. Fig. 1, shows that the microstructure of the weld is smooth with minute grain sizes. The boundary layers appear to be well overlapped. Fig. 2 shows a combination of minute and few large grain sizes. Most of the grain boundaries are well overlapped. However, for Fig. 3, the microstructure appears to have been affected by the introduction of air entrance in large amounts. The grains appeared to be brittle and large. This condition tends to accommodate gas entrapment in the weld before it eventually solidifies.

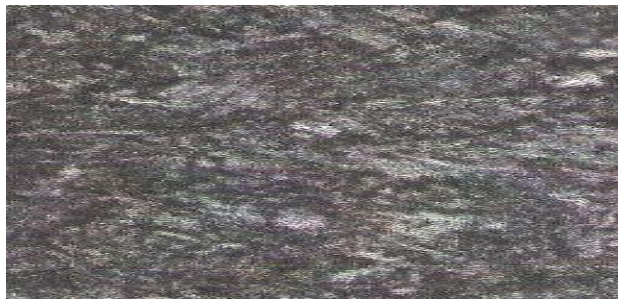


Fig. 1. Weld Microstructure made from the horizontal position.



Fig. 2. Weld Microstructure made from the vertical position.



Fig. 3. Weld Microstructure made from the overhead position.

4. Conclusion

The cooling rates from the welding process that took place at the horizontal, vertical and overhead positions were determined in this study. Also the corresponding effects of the cooling pattern on the weld microstructure were also examined. From the results, it can be concluded that the welding process made at the horizontal position produced weld microstructure that possess the best quality. This indicates that the cooling rate obtained in this position is just adequate for the welding process.

References

Achebo, J. I., 2008. Development of Aluminium Welding Flux from Local Raw Materials. PhD Thesis, Department of Production Engineering, University of Benin, Nigeria.

Atkins, G., Thiessen, D., Nissley, N., Adonyi, Y., 2002. Welding process effects in weldability testing of steels. *Welding Journal*, 4, Pp. 61s-68s.

Bhadeshia, H.K.D.H., Svensson, L.E., 1993. In *Mathematical Modeling of Weld Phenomena* (ed. K.E Easterling and H.K.D.H Bhadeshia). Institute of Materials, London, pp 109-182.

De, A., Walsh, C.A., Maiti, S.K., Bhadeshia, H.K.D.H., 2003. Prediction of cooling rate and microstructure in laser spot welds. *Science and technology of Welding and Joining*, 8, 6. 391-399.

Hess, W.F., Merrill, L.L., Nippes, E.E., Jr., Bunk, A.P., 1943. The measurement of cooling rates associated with arc welding and their application to the selection of optimum welding conditions. *Welding Journal*, 22 (9), 377s – 422s.

Ion, J.C., Easterling, K.E., Ashby, M.F., 1984. A second report on diagrams of microstructure and hardness for heat affected zones in welds. *Acta Metall.*, 32 (11), 1949 – 1962.

Okui, N., Etron, D., Bordelon, F., Hirata, Y., Clark, G., 2007. *Weld. J.* 86, 2, p. 35s – 43s.

Poorhaydari, K., Patchett, B.M., Ivey, D.G., 2005. Estimation of cooling rate in the welding of plate with intermediate thickness. *Welding Journal*, 10, 149s-155s.

Rosenthal, D., 1946. The theory of moving sources of heat and its application to metal treatments. *Trans. ASME*, 48:848-866.

Yang, Z. Debroy, T. 1999. Modeling macro and microstructures of gas metal arc welded HSLA-100 steel. *Metall. and Mater. Trans B*, Vol. 30B, pp 483-493.